



Impact of environmental forcing on the acoustic backscattering strength in the equatorial Pacific: diurnal, lunar, intraseasonal, and interannual variability

Marie-Hélène Radenac, P. E. Plimpton, Anne Lebourges-Dhaussy, L. Commien, M. J. Mcphaden

► To cite this version:

Marie-Hélène Radenac, P. E. Plimpton, Anne Lebourges-Dhaussy, L. Commien, M. J. Mcphaden. Impact of environmental forcing on the acoustic backscattering strength in the equatorial Pacific: diurnal, lunar, intraseasonal, and interannual variability. Deep Sea Research Part I: Oceanographic Research Papers, 2010, 57 (10), pp.1314-1328. 10.1016/j.dsr.2010.06.004 . ird-00544133

HAL Id: ird-00544133

<https://hal.ird.fr/ird-00544133>

Submitted on 7 Dec 2010

HAL is a multi-disciplinary open access archive for the deposit and dissemination of scientific research documents, whether they are published or not. The documents may come from teaching and research institutions in France or abroad, or from public or private research centers.

L'archive ouverte pluridisciplinaire **HAL**, est destinée au dépôt et à la diffusion de documents scientifiques de niveau recherche, publiés ou non, émanant des établissements d'enseignement et de recherche français ou étrangers, des laboratoires publics ou privés.

Manuscript Number: DSR1-D-09-00173R1

Title: Impact of environmental forcing on the acoustic backscattering strength in the equatorial Pacific: diurnal, lunar, intraseasonal, and interannual variability

Article Type: Regular Manuscript

Keywords: biological-physical interactions; equatorial Pacific; sound scattering; micronekton; ADCP moorings

Corresponding Author: Dr. Marie-Hélène Radenac,

Corresponding Author's Institution: LEGOS

First Author: Marie-Hélène Radenac

Order of Authors: Marie-Hélène Radenac; Patricia E Plimpton; Anne Lebourges-Dhaussy; Ludivine Commien; Michael J McPhaden

Abstract: We analyzed several records of mean volume backscattering strength (Sv) derived from 150 kHz Acoustic Doppler Current Profilers (ADCPs) moored along the equator in upwelling mesotrophic conditions and in the warm pool oligotrophic ecosystem of the Pacific Ocean. The ADCPs allow for gathering long time-series of non-intrusive information about zooplankton and micronekton at the same spatial and temporal scales as physical observations. High Sv are found from the surface to the middle of the thermocline between dusk and dawn in the mesotrophic regime. Biological and physical influences modified this classical diel cycle. In oligotrophic conditions observed at 170°W and 140°W during El Niño years, a subsurface Sv maximum characterized nighttime Sv profiles. Variations of the thermocline depth correlated with variations of the base of the high Sv layer and the subsurface maximum closely tracked the thermocline depth from intraseasonal to interannual time-scales. A recurring deepening (20 to 60 m) of the high Sv layer was observed at a frequency close to the lunar cycle frequency. At 165°E, high day-to-day variations prevailed and our results suggest the influence of moderately mesotrophic waters that would be advected from the western warm pool during westerly wind events. A review of the literature suggests that Sv variations may result from changes in biomass and species assemblages among which myctophids and euphausiids would be the most likely scatterers.

Impact of environmental forcing on the acoustic backscattering strength in the equatorial Pacific: diurnal, lunar, intraseasonal, and interannual variability

Marie-Hélène Radenac^{a,b}, Patricia E. Plimpton^c, Anne Lebourges-Dhaussy^d, Ludivine Commien^a, Michael J. McPhaden^c

^a Université Paul Sabatier; Laboratoire d'Etudes en Géophysique et Océanographie Spatiales; 14 Av, Edouard Belin, F-31400 Toulouse, France

^b Institut de Recherche pour le Développement, Toulouse, France

^c NOAA Pacific Marine Environmental Laboratory, Seattle, Washington, USA

^d Institut de Recherche pour le Développement de Bretagne, Plouzané, France

Corresponding author: Marie-Hélène Radenac; marie-helene.radenac@legos.obs-mip.fr; LEGOS, 14 avenue Edouard Belin, F-31400 Toulouse, France; telephone: 33 561333000; fax: 33 561253205;

Abstract

We analyzed several records of mean volume backscattering strength (S_v) derived from 150 kHz Acoustic Doppler Current Profilers (ADCPs) moored along the equator in upwelling mesotrophic conditions and in the warm pool oligotrophic ecosystem of the Pacific Ocean. The ADCPs allow for gathering long time-series of non-intrusive information about zooplankton and micronekton at the same spatial and temporal scales as physical observations. High S_v are found from the surface to the middle of the thermocline between dusk and dawn in the mesotrophic regime. Biological and physical influences modified this classical diel cycle. In oligotrophic conditions observed at 170°W and 140°W during El Niño years, a subsurface S_v maximum characterized nighttime S_v profiles. Variations of the thermocline depth correlated with variations of the base of the high S_v layer and the

subsurface maximum closely tracked the thermocline depth from intraseasonal to interannual time-scales. A recurring deepening (20 to 60 m) of the high S_v layer was observed at a frequency close to the lunar cycle frequency. At 165°E, high day-to-day variations prevailed and our results suggest the influence of moderately mesotrophic waters that would be advected from the western warm pool during westerly wind events. A review of the literature suggests that S_v variations may result from changes in biomass and species assemblages among which myctophids and euphausiids would be the most likely scatterers.

Keywords: biological-physical interactions; equatorial Pacific; sound scattering; micronekton; ADCP moorings

1. Introduction

The range of influences of zooplankton and micronekton (crustaceans, molluscs, fish of 1 to 10 cm length) on biogeochemistry is wide. These include the impact on nutrient cycling through the relative magnitude of ingestion and excretion, export of inorganic and organic matter by migrating organisms (Longhurst et al., 1989; Dam et al., 1995; Steinberg et al., 2002), and influence on the distribution of top predators because they largely feed on micronekton (Lehodey et al., 2010).

In the open ocean, distributions of zooplankton and micronekton vary over a broad range of spatial and temporal scales in response to biological and environmental controls (Folt and Burns, 1999). Diel vertical migration is commonly observed in many mesozooplankton (200-2000 μm) or micronekton species. Organisms rise toward the surface at dusk and swim to deeper waters at dawn. A “reverse migration” pattern is also observed (ascent at dawn and descent at dusk) for some species as well as many intermediate migrating behaviors. These

general upward or downward movements of mixed species populations are influenced by
 environmental (light, temperature) and/or biological (endogenous cycle, food availability,
 predator avoidance, population composition) factors (Haney, 1988; Folt and Burns, 1999).
 Discriminating the impact of different mechanisms is difficult because they often interact. In
 particular, the light level and predation pressure are linked as mortality due to visual predation
 is reduced when the light level is low in the surface layer where food is available (Gliwicz,
 1986). In general, diel vertical migration can be seen as a strategy for organisms to escape
 visual predators at depth during the day and feed in the surface layer during the night.

Light is considered as the major factor that triggers diel vertical migration. In the classical
 migration pattern, the timing of upward (downward) movement is modulated by the length of
 day (Fisher and Visbeck, 1993; Asjian et al., 2002; Jiang et al., 2007). Reduced amplitude of
 downward migrations have been observed on cloudy days (Pinot and Jansá, 2001; Ashjian et
 al., 2002). Moonlight also modulates the vertical migration patterns. Some micronekton
 organisms stop their upward migration and do not reach the surface layer or dive slowly after
 dusk when moonlight is bright; abundance of some species may also increase because of the
 decrease of predation pressure (Legand et al., 1972; Roger, 1974; Gliwicz, 1986; Hernández-
 León, 1998; Tarling et al., 1999, Pinot and Jansá, 2001). Interestingly, during the night of an
 eclipse, animals did not descend until the end of the umbra (the time that the moon is in the
 Earth's shadow) (Tarling et al. 1999). Possible interactions of external factors with
 endogenous rhythm have been mentioned by Velsch and Champalbert (1994) and Tarling et
 al. (1999). Physical structures such as fronts, eddies, stratification variations may also alter
 the characteristics of the diel migration patterns at different spatial and temporal scales
 (Marchal et al., 1993; Fielding et al., 2001; Wade and Heywood, 2001; Vélez-Belchi et al.,
 2002).

76

77 Diel migration behavior has been observed using net sampling (for example: Roger, 1974;
 78 Longhurst et al., 1989; Le Borgne and Rodier, 1997) by contrasting day and night
 79 measurements, and time-series derived from repeated cruises allowed for studying seasonal
 80 and interannual variability (Madin et al., 2001). Generally, episodic events and fine vertical
 81 distribution cannot be resolved over long periods of time because of sampling constraints.
 82 Acoustic devices have allowed for monitoring animals' behavior at fine vertical and temporal
 83 resolution as they detect targets mainly composed of zooplankton and micronekton organisms
 84 at frequencies on the order of 100 kHz (Ressler, 2002). Following Plueddemann and Pinkel
 85 (1989), acoustic studies (for example, Fisher and Visbeck, 1993; Heywood, 1996; Kaneko et
 86 al., 1996; Tarling et al., 1999; Pinot and Jansá, 2001; Asjian et al., 2002; Jiang et al., 2007)
 87 have described the characteristic alternate pattern of low and high backscattering during the
 88 day and night, and their modulations. Since Schott and Johns (1987), many studies used
 89 moored Acoustic Doppler Current Profilers (ADCPs) to describe seasonal variations of diel
 90 migration, including periods of rough conditions, and how they are affected by variations in
 91 light intensity or other physical forcing (Fisher and Visbeck, 1993; Flagg et al., 1994; Asjian
 92 et al., 1998; Pinot and Jansá, 2001).

93

94 Equatorial Pacific ecosystems reflect different physical forcing and characteristics. The
 95 western basin is occupied by warm, fresh, and oligotrophic nitrate depleted surface waters
 96 (Fig. 1a). In this region, sea surface temperature (SST) is higher than 29°C, sea surface
 97 salinity lower than 35, and surface chlorophyll lower than 0.1 mg m⁻³. The nitracline and the
 98 subsurface chlorophyll maximum are closely associated with the thermocline depth (Radenac
 99 and Rodier, 1996; Mackey et al., 1997; Navarette, 1998). The ocean variability is
 100 characterized by intraseasonal scales related to westerly wind variability and by interannual

scales related to the El Niño Southern Oscillation (ENSO) (McPhaden, 1999; 2004). East of the warm pool, equatorial upwelling brings cooler and saltier waters toward the surface in a huge region spreading westward from the South American coast. Although the surface nitrate concentration is high, the chlorophyll content remains moderate (less than 0.25 mg m^{-3} on average between 1999 and 2004) because of an iron-limited and grazing-balanced ecosystem (Landry et al., 1997). Variability occurs at intraseasonal (tropical instability waves, equatorial Kelvin waves), seasonal, and ENSO time-scales. The sharp salinity front at the limit between the warm pool and the cold tongue (Kuroda and McPhaden, 1993) also marks the discontinuity of chemical and biological properties (Rodier et al., 2000) between the oligotrophic and mesotrophic ecosystems. Small zooplankton (35-200 μm) biomass is not significantly different in the oligotrophic and mesotrophic regions whereas the mesozooplankton biomass is higher (e.g., 2.5-fold increase in September-October 1994) in the mesotrophic system (Le Borgne and Rodier, 1997). Little is known about micronekton biomass and behavior along the equator. Population dynamics model results show that the zonal distribution of the micronekton biomass in the 0-100 m layer increases from the warm pool to the cold tongue (Lehodey et al., 2010) and intriguingly, highest tuna catch in the Pacific occur on the oligotrophic warm pool side of the front (Lehodey et al., 1997).

Subsurface ADCP moorings are typically deployed within 5-15 kms of several equatorial Autonomous Temperature Line Acquisition System (ATLAS) moorings of the Tropical Atmosphere Ocean/Triangle Trans Ocean Buoy Network (TAO/TRITON) (McPhaden et al., 1998). They are used to monitor the variability of the equatorial Pacific current system, but they also provide long time-series of mean volume backscattering strength (S_v). Although temperature, salinity, current, and meteorological data are widely used in the oceanography community, S_v has not yet been used for biological purposes. Such long records are a unique

opportunity to monitor perturbations of the diel migration at the same vertical and temporal scales as physical variables. In this study, we describe the variability of the acoustic backscattering signal at three equatorial sites (165°E, 170°W, 140°W) located in both equatorial ecosystems (Fig. 1a). Our objective is to investigate whether the response of the ADCP signal in terms of magnitude and diel vertical migration pattern is specific to each ecosystem. We also discuss the impact of environmental factors (moonlight and stratification) in both ecosystems at the lunar, intraseasonal, and interannual timescales.

2. Data and processing

2.1. The ADCP data

We have selected a subset of data in order to describe the biomass signals in the oligotrophic warm pool and in the mesotrophic upwelling region under the influence of different physical conditions. Processing of the data for the purposes of this study is very labor intensive. Therefore, we have focused on recent records at three equatorial sites of the TAO/TRITON array: November 2001-November 2003 at 165°E, July 2002-July 2004 at 170°W and September 1996-September 1999 at 140°W during the strong 1997-1998 El Niño and subsequent La Niña. Instruments are 153.6 kHz RDI narrowband ADCPs mounted in an upward-looking configuration at nominal depths of 250 to 300 m on subsurface moorings (Plimpton et al., 2004). Data in the upper 40 m “deadzone” are excluded because of contamination from reflections off the sea surface. Moorings are recovered and replaced with new instruments approximately once per year (Table 1).

The equation of the mean volume backscattering strength (RDI, 1990), S_v in decibels, can be rearranged into four components:

$$S_v = 10 \log_{10} \left[\frac{4.47 \times 10^{-20} K_2 K_s (T_x + 273.18)}{c P K_1} \right] + 20 \log_{10} R + 2 \alpha R + 10 \log_{10} \left[10^{K_c (E_a - E_r)/10} - 1 \right]$$

The first component combines system dependant variables: K_2 is the system noise factor, K_s is a constant that depends on ADCP frequency, K_1 is the power transmitted into the water (watts), c is the speed of sound (m s^{-1}) at the scattering layer being measured, T_x is the temperature of the transducer ($^{\circ}\text{C}$) recorded by the ADCP, and P is the transmit pulse length (m). The second and third components account for beam spreading and absorption, respectively. R is the range along the beam to the scatterers (m) and α is the absorption coefficient in seawater (dB m^{-1}). We used the Francois and Garrison (1982) equation to calculate α which is a function of temperature, salinity, sound frequency, depth, and pH. Since temperature and salinity profiles are not continuously available from the moorings, we calculated mean α profiles for each deployment and assumed a constant pH value of 8.1 which is sufficient in the buffered seawater. The last component represents the volume scattering strength of the water mass. E_a is the echo intensity (counts) measured by the ADCP, E_r is the background reference noise value (counts) taken as the minimum value measured for each beam during each deployment, and K_c is a conversion factor (dB counts^{-1}).

In the following study, we present the mean S_v of the four beams (the antilog value of S_v was taken before averaging). For most deployments, S_v offset of each beam (relative to the mean S_v profile of the four beams) was less than 1 dB. However, at 165°E , offsets of about 1.5 dB and -2 dB were detected for beams 1 and 4 during deployment wa3, and 1.16 dB for beam 2 during deployment wa4. In such cases, the offset was removed from S_v before averaging. In order to study variations in the diel vertical migration associated with environmental forcing at different time scales, we constructed nighttime (daytime) S_v profiles by averaging S_v

profiles within 2 hours of midnight (noon). Note that ADCPs are not calibrated and uncertainty remains in comparing S_v between moorings.

2.2. Other data

We use additional *in situ* and satellite data to set up the environmental context. Although the conversion ratio between the carbon biomass and chlorophyll (C:Chl) varies (Wang et al., 2009), surface chlorophyll can be used as a realistic index of the trophic conditions. Surface chlorophyll concentrations are SeaWiFS version 4, 9 km, 8-day composites computed by the NASA Goddard Space Flight Center (GSFC) Distributed Active Archive Center (DAAC) (McClain et al., 2004). Weekly SST are retrieved from the Tropical Rainfall Measuring Mission (TRMM) Microwave Imager (TMI) starting in December 1997 and from the Reynolds et al. (2002) *in situ* and satellite analysis before that date. Depths of the 29°C ($Z_{29^\circ\text{C}}$) and 20°C ($Z_{20^\circ\text{C}}$) isotherms are derived from daily temperature profiles recorded at the TAO/TRITON equatorial moorings. We also use daily SST, ADCP currents, wind speed, and short-wave solar radiation from the moorings. When TAO/TRITON winds are missing, we use the weekly QuickSCAT wind speed retrieved from the SeaWind scatterometer and delivered by CERSAT, IFREMER. Phases of the moon and times of sunrise and sunset originate from the web site of the US Naval Observatory (<http://aa.usno.navy.mil/>).

3. Results: the backscattering strength at the three sites

The TAO/TRITON mooring time-series that we use are from the central (140°W) and the western part (170°W) of the mesotrophic ecosystem, and the eastern part of the oligotrophic warm pool (165°E) (Fig. 1a). In this chapter, we first set the context by describing the large scale physical dynamics and ecosystem variability. Then, we report S_v time-series

representative of conditions encountered at each mooring and describe the main types of diurnal migration and perturbations under the influence of the physical environment.

199

3.1. The large scale context

The frontal zone between the oligotrophic and mesotrophic ecosystems closely follows the 0.1 mg m⁻³ surface chlorophyll isoline (Murtugudde et al., 1999; Stoens et al., 1999; Fig. 1a). Its longitudinal location varies mainly at the El Niño Southern Oscillation (ENSO) time-scale (Murtugudde et al., 1999; Radenac et al., 2001; Le Borgne et al., 2002; Ryan et al., 2002; Radenac et al., 2005) as can be seen from the evolution of satellite-derived chlorophyll in the equatorial Pacific (Fig. 1b). During El Niño years, oligotrophic waters of the warm pool spread eastward. The front reached 160°W during the moderate 2002 El Niño event and 130°W during the peak period of the major 1997 event. Very low chlorophyll values (< 0.07 mg m⁻³), such as those found in the subtropical gyres (McClain et al., 2004), were confined in the eastern part of the warm pool. Further west, surface chlorophyll and biological production were higher than during non-El Niño years (Dandonneau, 1986; Mackey et al., 1997; Turk et al., 2001) and episodic increases of surface chlorophyll were associated with westerly wind events (Siegel et al., 1995; Radenac et al., unpublished results). The thermocline, represented here by the depth of the 20°C isotherm (Kessler, 1990), was uplifted in the western Pacific warm pool and depressed in the cold tongue (Fig. 1c) in 1997 and 2002. During the period of the study, equatorial downwelling Kelvin waves were forced in the western basin by intraseasonal westerlies and propagated eastward. They depressed the thermocline and initiated eastward displacements of the front, particularly in December 1996, March 1997, December 2001, the second half of 2002, December 2003, and the second half of 2004 (Fig. 1c).

During La Niña events, the equatorial cold tongue extends westward as observed during the long-lasting La Niña period between mid 1998 and 2001 when chlorophyll-rich waters expanded west of 170°E (Fig. 1b). In mid-1998, the chlorophyll bloom was the strongest and largest observed by SeaWiFS in the central and eastern equatorial Pacific. This unusually strong manifestation of interannual variability following the major 1997-1998 El Niño event resulted from strong vertical macro- and micro-nutrient fluxes associated with the surfacing of the Equatorial Undercurrent (EUC) and thermocline outcropping (Chavez et al., 1999; Ryan et al., 2002). The thermocline depth remained shallower than climatological values until early 2000 (Fig. 1c).

3.2. 170°W

The 0°, 170°W mooring was situated at the western end of the cold mesotrophic tongue (SST < 29°C, surface chlorophyll $\approx 0.2 \text{ mg m}^{-3}$) except from September to December 2002 when the eastern edge of the oligotrophic warm pool migrated past 170°W during the mild El Niño event (Fig. 1b; Fig. 2a). At this mooring as well as at the two other sites, the dominant S_v variability occurs at the diurnal frequency. The two records we present (Table 1) allow contrasting observations of the diurnal migration in two ecosystems at this site.

3.2.1. Diel cycles

Diel cycles in early June 2003 (Fig. 3a) are representative of those encountered in mesotrophic cold tongue conditions that lasted from February 2003 to June 2004 (Fig. 2). The mean nighttime S_v profile was fairly homogeneous above $Z_{20^\circ\text{C}}$ and decreased below (Fig. 3b). Daytime S_v was more homogeneously distributed over the observed layer. As a consequence, the averaged difference between the nighttime and daytime S_v was about 10 dB above $Z_{20^\circ\text{C}}$ (Table 2) while it was slightly negative below. The characteristic alternate pattern of low

daytime S_v and high nighttime S_v in the upper layer reflects the migratory behavior of zooplankton and micronekton organisms that rise from below the transducer depth at dusk and descend at dawn.

Between September and December 2002, the 170°W mooring was in the oligotrophic warm pool. Vertical S_v distribution exhibited several distinctive features compared to S_v profiles in mesotrophic conditions. The first one was a S_v decrease (5 to 10 dB) above $Z_{20^\circ\text{C}}$ nighttime or daytime. The difference between night and day S_v above $Z_{20^\circ\text{C}}$ tended to be lower in the oligotrophic system than in the mesotrophic one (Fig. 3b, d; Table 2). The second remarkable feature was an alteration of nighttime profiles (Fig. 2b) characterized by a subsurface maximum located in the upper part of the thermocline (Fig. 3d) that did not persist during daytime. The depth of the subsurface S_v maximum deepened concurrently with $Z_{20^\circ\text{C}}$ and $Z_{29^\circ\text{C}}$ in early September, mid-October, and mid-December (Fig. 2b) when three downwelling Kelvin waves passed the 170°W mooring while oligotrophic conditions prevailed (Fig. 1c). The correlation coefficient between the depth of the subsurface S_v maximum and $Z_{20^\circ\text{C}}$ between 10 September and 31 December 2002 is 0.77 ($p < 0.01$), suggesting a significant influence of changes in stratification on S_v . The correlation relative to $Z_{29^\circ\text{C}}$ yields $r = 0.87$ ($p < 0.01$). Moon light is also a significant influence on S_v as discussed below.

3.2.2. The lunar cycle

The influence of the lunar cycle is clearly seen in the time-series of nocturnal S_v between February 2003 and June 2004 (Fig. 2b) during mesotrophic conditions. During full moon periods, S_v decreased in the surface layer and high S_v values extended deeper into the thermocline by 20 to 30 m. As expected from these observations, a strong peak at the frequency closest to the frequency of the lunar cycle (frequency of 0.034 cpd) dominates S_v

power spectra (not shown). Little energy was found between 70 and 120 m while maximum energy was observed between 150 and 200 m. Unfortunately, data above 40 m depth were unavailable and only the lower part of a high energy surface layer was captured above 60 m. During full moon periods, S_v decreased sharply by 5 to 10 dB at the bottom of the surface layer (40 m; Fig. 4a) while the range of increases in the middle of the thermocline was larger (Fig. 4b).

Such variations can be assessed by examining S_v diel cycles during a representative lunar cycle (Fig. 5). We chose September 2003 because short wave radiation measured at the TAO/TRITON mooring during the day was high (not shown). Therefore, although it tends to be cloudier and rainier over the tropical oceans at night compared to during the day (Serra and McPhaden, 2004), we might expect nighttime cloudiness at this time and location to be relatively low. Sunset is around 1800 local time (LT) and sunrise is around 0600 LT. At new moon, the moon and sun rise together (27 August and 26 September) while at full moon, the moon rises when the sun sets (9 September).

Diel cycles surrounding new moon (26-27 August, 25-26 September) exhibited a “classical” pattern with a rapid vertical ascent at sunset. High S_v levels extended from 40 m depth to the middle of the thermocline until sunrise. Between new moon (26-27 August) and full moon (9-10 September), duration of period between moonset and sunrise decreased. S_v in the surface layer was lower at the beginning of the night when moonlight was bright than when moonlight became dimmer. On the full moon night (9 September), surface S_v decreased after the swift vertical upward migration at dusk. During the following days, the nighttime descent happened later in the night. As a consequence, duration of observation of high S_v in the surface layer was longer around new moon than around full moon. At depth, the high S_v layer

tended to go deeper during the early hours of the night preceding full moon while it deepened at the end of the night after full moon, leading to asymmetrical patterns over the night.

Although it is not as clear as in the mesotrophic regime, examination of individual daily S_v in the oligotrophic regime cycles suggests that the lunar cycle influenced the vertical distribution in the upper layer and the depth of the subsurface maximum layer (not shown). Following full moon, a surface decrease and a deepening of the subsurface S_v maximum was often observed after moonrise. Before full moon, surface S_v increased during darkness following moonset. Yet, time-series in oligotrophic ecosystems encompassed only three lunar cycles (see Fig. 2b) and no definitive conclusion can be drawn from this data set.

3.3. 140°W

Situated in the central equatorial Pacific, the mooring at 140°W experienced very unusual ecosystem and stratification conditions during the major 1997 El Niño and 1998 La Niña events (McPhaden, 1999; Strutton and Chavez, 2000; Radenac et al., 2001). During the pre-El Niño period (September 1996 - September 1997), the ecosystem was mesotrophic with surface chlorophyll measured by the Ocean Color and Temperature Scanner (OCTS) and Polarization and Directionality of the Earth Reflectances (POLDER) mission between November 1996 and June 1997 around 0.15 mg m^{-3} (Radenac et al., 2001; Ryan et al., 2002). SST was close to climatology in 1996 and increased in 1997 as the El Niño event proceeded (Fig. 6a). S_v patterns were close to those encountered in the mesotrophic regime at 170°W with high nighttime S_v above $Z_{20^\circ\text{C}}$. The thermocline depth was close to climatology in late 1996 after which two downwelling Kelvin waves depressed the thermocline by more than 20 m in January and March 1997 (Fig. 1c; Fig. 6b). The depth of the high nighttime S_v layer followed $Z_{20^\circ\text{C}}$ variations (Fig. 6b) during the pre-El Niño period and during the passage of

the downwelling Kelvin waves. Correlation coefficient between the depth of the high nighttime S_v layer (represented by the -58 dB isoline) and $Z_{20^\circ\text{C}}$ (removing short time scale variations with a 15-day-Hanning filter) is 0.84 ($p < 0.01$). During this period, variations at the lunar frequency (Fig. 6b) were comparable to observations in the 170°W mesotrophic ecosystem. The power spectrum peaked in the surface layer and at the base of the high nighttime S_v layer (not shown).

During the peak of the El Niño event (October 1997 - January 1998), waters of the oligotrophic warm pool reached 140°W (Fig. 6a; Chavez et al., 1999; Strutton and Chavez, 2000; Radenac et al., 2001). Accordingly, the lowest S_v were observed in November-December (Fig. 6a, b). The vertical structure changed. Adjustment from a uniform nighttime high S_v layer to oligotrophic type profiles with a nighttime S_v maximum squeezed between $Z_{29^\circ\text{C}}$ and $Z_{20^\circ\text{C}}$ was swift. Narrowing of the low nighttime S_v layer above $Z_{29^\circ\text{C}}$ and shoaling of the underlying layer of maximum S_v were significant features of the period. They closely followed the shoaling of the thermocline (Fig. 1c). As for the 170°W time-series, surface decreases were observed during full moon and there were hints of deepening of the subsurface S_v maximum in November and December 1997 (not shown).

Following the strong El Niño event, the sudden recovery of trade winds triggered an abrupt onset of La Niña conditions. Unusually shallow thermocline ($Z_{20^\circ\text{C}}$ was only 30 m deep; Fig. 6b) and high surface chlorophyll (almost fourfold the average value of 0.21 mg m^{-3}) prevailed between June and August 1998 (Fig. 6a). During this “shallow mesotrophic” period, the highest nighttime S_v were trapped above $Z_{20^\circ\text{C}}$ in the upper 40 m layer where the ADCP signal is missing (Fig. 6b; Fig. 7). During the mid-1998 bloom period, a high S_v layer was located below $Z_{20^\circ\text{C}}$ during the day (Fig. 6c). It sank gradually from sunrise to noon then rose toward

the surface until sunset (Fig. 7). Above 200 m, it merged with rapid vertical migrating layer from below the transducer. The nighttime surface decrease associated with full moon period was not observed, but some increases were observed from $Z_{20^{\circ}\text{C}}$ to the bottom of the sampled layer (Fig. 6b) for a few cycles (September 1998-April 1999).

3.4. 165°E

S_v data at 165°E exhibits high frequency variability (Fig. 8) that possibly reflects the special location of the mooring close to the frontal zone between the oligotrophic and mesotrophic ecosystems (Fig. 1b). Although, the mooring was situated in surface chlorophyll poor waters in January-June 2002, January-March 2003, and July-November 2003 (Fig. 8a), oligotrophic type profiles with a subsurface nighttime S_v maximum were observed only in January-February 2003; during the other periods of time, the day to day variability was high, with vertical distribution suggesting oligotrophic or mesotrophic type profiles, or numerous intermediate vertical patterns.

During the second half of 2002, El Niño conditions developed with repeated westerly wind events (WWE; Fig. 8a), eastward equatorial surface currents (Fig. 8d), shoaling of the thermocline (Fig. 1c), and modest increases of surface chlorophyll to about 0.1 mg m^{-3} (Fig. 8a). S_v profiles showed relatively high nighttime values in the warm isothermal layer (above $Z_{29^{\circ}\text{C}}$). Variability was high and transient intermediate patterns between oligotrophic and mesotrophic configurations were also observed. The successive WWE gave rise to easterly equatorial surface currents (Fig. 8). Interestingly, nighttime S_v above $Z_{29^{\circ}\text{C}}$ increased to around -54 dB when the zonal current was eastward while it was around -58 dB at the beginning of the year (Fig. 9a) suggesting that a water mass with different chlorophyll content and micronekton properties was advected from the west during El Niño. The relative minima

in June 2002 and February 2003 corresponded to the occurrence of very oligotrophic waters around the mooring. The increase in S_v after March 2003 (Fig. 9) was related to the westward extent of the mesotrophic ecosystem that reached the mooring site (Fig. 1b).

Some S_v decreases during full moon nights were observed in the surface layer after July 2002 (Fig. 8b). They were simultaneous with deepening of the base of the nighttime high S_v layer. Although this pattern is not always clear by visual examination, power spectral analysis captures it with the highest energy in the vicinity of $Z_{20^\circ\text{C}}$ and a moderate energy layer above 100 m (not shown).

4. Discussion

4.1. ADCP detection range

ADCPs in an upward-looking configuration involve a “deadzone” near the air/sea boundary where separating between targets and surface signal is not possible (Ona and Mitson, 1996) because of contamination from sidelobe reflections. We set the deadzone for the moored TAO/TRITON ADCPs at about 40 m. Also, the depths of the transducers are between 250 and 300 m (Plimpton et al., 2004). So, overall, the detection range is limited to a 40-250 m layer. Micronekton organisms may be divided into epipelagic (above 150 m) and mesopelagic (150-1000 m) groups (Roger, 1971; Legand et al., 1972; Legendre and Rivkin, 2005). Migrant species move at night from deep layers toward more superficial layers. Therefore, equatorial ADCPs sample a great part of the epipelagic layer. Nighttime biomass derived from net samples is high above depths of 100 to 200 m and high S_v have been observed above 50 m in the warm pool (Kaneko et al., 1996) and in different sites of the world ocean (Tarling et al., 1999; Wade and Heywood, 2001; Pinot and Jansá, 2001). So, the deadzone limitation prevents us from monitoring 20 to 40% of the high biomass layer. In particular, we are not

able to describe thoroughly the vertical distribution in oligotrophic conditions (some situations suggest a high S_v layer above 40 m) and we miss the high S_v layer during the 1998 bloom at 140°W. Nonetheless, for that part of the water column we do observe, the sampling is continuous and highly resolved in the vertical.

4.2. Sources of scattering

Zooplankton and micronekton targets are responsible for a great part of the backscattering signal at frequencies of the order of 10^2 kHz (Wiebe et al., 1990). Typically, this backscattering is determined by the product of the wave number for the sound ($k = 2\pi/\lambda$) times the scatterer size (a) expressed as an equivalent radius. In the Rayleigh domain ($ka \ll 1$), the signal increases strongly with the frequency (or the size) until a transition zone around $ka = 1$, and then the scattering enters in the geometric domain ($ka \gg 1$), where the signal is non-monotonic (Holliday and Pieper, 1995). For a 150 kHz ADCP, the transition zone corresponds to organisms of size around 1 cm at the smallest. Nevertheless, the backscattering is related to the sound frequency used and to the size, shape, orientation, and physical properties of the targets (Stanton et al., 1994; McGehee et al., 1998). Because it is not possible to discriminate between variations in size and in abundance with single-frequency techniques, Holliday and Pieper (1995) reviewed optimal conditions to estimate abundance. In particular, they pointed out that a single organism should dominate the acoustic scattering and predicting the animal target strength with an appropriate acoustic scattering model would help interpreting the single-frequency signal. Yet, zooplankton and micronekton populations are usually composed of a complex assemblage of species that complicates the interpretation of S_v in terms of biologically relevant quantities. For instance, efficient sound scatterers (pteropods, siphonophores, fish) may strongly contribute to S_v although their abundance or biomass is low at specific depths and locations (Wiebe et al., 1996; Fielding et al., 2004; Mair

et al., 2005; Lavery et al., 2007; Lawson et al., 2008). In particular, gas-bearing siphonophores were responsible for the strong scattering layer observed at 120 kHz in the seasonal thermocline in the Gulf of Maine (Lavery et al., 2007). Pelagic fish that can dominate the acoustic scattering at 150 kHz, probably do not strongly alter the signal because of their patchiness and scarcity (Plimpton et al., 1997; Lawson et al., 2008). Changes in the taxonomic composition (relative contribution of euphausiids, amphipods, myctophids, and copepods) explained most of changes in S_v over three zones in the northeast Atlantic (Wade and Heywood, 2001). Similarly, Ashjian et al. (1998) associated the occurrence or absence of diel vertical migrations to various species advected with water masses. Other factors such as size or orientation that vary between species and within species can further confound the interpretation of S_v . Different vertical migration patterns related to sizes of animals at larval or post-larval stages (Munk et al., 1988; León et al., 2008) and the size increase along the year may impact S_v variability at seasonal or longer time scales. Different species assemblages during day and night also affect S_v diel cycle. For example, Ballón Soto (2010) observed a mean size increase of about 5% during the night in the epipelagic layer of the Humboldt Current System, indicative of the migration of larger animals from deeper layers. In addition, animal orientation probably influences nighttime and daytime S_v as this orientation changes among species and seems to differ according to behaviors such as migration or feeding (Warren et al., 2002; Fielding et al., 2004).

No concurrent echo-sounder measurements or net samples were available for this study to constrain the complex interpretation of single-frequency S_v . Therefore, we relied on a review of the literature to identify likely scatterers in the equatorial Pacific. Several zooplankton and micronekton species have been identified as possible migrating scatterers in the 10s to 100s kHz range. Copepods and pteropods contributed most to the 420 kHz S_v on Georges Bank

(Wiebe et al., 1996). Migrating layers at 150 kHz were composed of euphausiids, amphipods, myctophids, and copepods in the northeast Atlantic (Wade and Heywood, 2001); myctophids and euphausiids in the Mediterranean Sea (Tarling et al., 1999; Pinot and Janša, 2001; Fielding et al., 2001) and in the Gulf of Mexico (Ressler, 2002); and fish in the Arabian Sea (Ashjian et al., 2002). To our knowledge, only net samples were used to evaluate variations of biomass and taxonomic composition in the equatorial Pacific. The nighttime micronekton biomass in the 0-100 m layer was about 4 times higher than the daytime biomass in the central equatorial Pacific (Legand et al., 1972) while in the western part of the warm pool, micronekton nighttime biomass in the 0-200 m layer was almost 8 times higher than daytime biomass and peaked in the 80-120 m layer (Hidaka et al., 2003). Flagg and Smith (1989) proposed a linear relationship between $\log(DW/4\pi)$ and S_v with a slope around 0.1 (DW is the dry-weight biomass in mg m^{-3}). Following this assumption, a four-fold biomass increase corresponds to a 6 dB S_v increase which is the order of magnitude of the 5 to 10 dB difference between observed nighttime and daytime S_v . Actually, the range of slopes derived for different sites and scatterers populations (0.115, Flagg and Smith, 1989; 0.055, Batchelder et al., 1995; 0.085 and 0.055, Wade and Heywood, 2001) shows that such a relationship is not universal and should be used with caution. The night/day variation of the mesozooplankton biomass was much lower than that of micronekton biomass: about 25% (15%) higher nighttime in the mesotrophic (oligotrophic) ecosystem (Le Borgne and Rodier, 1997). In the central Pacific, migrant organisms were mainly fish among which myctophids were the most numerous, large (> 2 mm) euphausiids, cephalopods, and shrimp (about 30%, 17%, 11%, and 8%, respectively, of the biomass; Legand et al., 1972). Copepods and chaetognaths dominated the mesozooplankton biomass (Le Borgne and Rodier, 1997). In the western warm pool, myctophids dominated the nighttime biomass and, to a lesser extent, squids, euphausiids and shrimp (77%, 6.5%, 2.9%, and 2.8% of the biomass; Hidaka et al., 2003). Pteropods

represented a few percent of the micronekton (Legand et al., 1972) and of the mesozooplankton (Le Borgne and Rodier, 1997) biomass in both equatorial ecosystems. Comparable observations are reported for siphonophores (Legand et al., 1972; Le Borgne and Rodier, 1997), unfortunately, no information was given about possible gas inclusion.

4.3. Scattering variability in the equatorial Pacific

4.3.1. Oligotrophic and mesotrophic conditions

S_v records at the 170°W and 140°W sites show clear differences associated with the occurrence of oligotrophic or mesotrophic conditions. In mesotrophic conditions, nighttime (daytime) S_v was about 6 dB (4 dB) higher than in oligotrophic conditions (Table 2) which represent 4-fold (2.5-fold) biomass increases. S_v variations are highly consistent with mesozooplankton net measurements along the equator showing that the biomass tripled abruptly at the oligotrophic/mesotrophic limit (Le Borgne and Rodier, 1997). Comparison with micronekton biomass is less obvious. In the upper 200 m, nighttime biomass in the central equatorial Pacific (770 mg wet weight (WW) m⁻²; Legand et al., 1972) was lower than in the North Equatorial Counter Current (NECC) region of the western warm pool (1350 mg WW m⁻²; Hidaka et al., 2003). The ratio of daytime biomass between the warm pool and the central Pacific was about the same. Reasons for the discrepancy in variations between net samples and acoustic measurements are unclear. The S_v drop between mesotrophic and oligotrophic regimes does not necessarily reflect a biomass decrease but could result from different species assemblage seen in the preceding section. Another point could be that Hidaka et al. (2003) micronekton biomass in the nascent NECC is not representative of the very oligotrophic ecosystem of the eastern warm pool as chlorophyll concentrations slightly higher than 0.1 mg m⁻³ are recurrently observed in the NECC meanders (Christian et al., 2004; Messié and Radenac, 2006). However, nighttime biomass in

the very oligotrophic water of the North Equatorial Current would be 730 mg WW m^{-2} (Hidaka et al., 2003) which is the order of magnitude of the central Pacific biomass. These very few net samples suggest that micronekton biomass in the upper layer is higher (or of the same order of magnitude) in the oligotrophic than in mesotrophic conditions and does not explain S_v variations between the two ecosystems. The abrupt increase of the zooplankton biomass along the equator from oligotrophic to mesotrophic regimes evokes its possible influence on S_v , bearing in mind that zooplankton biomass represents more than 90% of the upper layer biomass (Legand et al., 1972). To be more conclusive, the influence of the taxonomic compositions on S_v in each ecosystem needs to be investigated.

Vertical S_v distributions within each ecosystem may reflect different species assemblages and migrating behavior. High nighttime S_v above the middle of the thermocline in mesotrophic conditions is consistent with the migration behavior of fish and large crustaceans that constitute most of the nighttime biomass in the 0-200 m layer (Legand et al., 1972). In the oligotrophic ecosystem, the S_v maximum in the upper part of the thermocline corresponds to the peak biomass situated between 80 and 120 m in net observations where myctophids represented more than 70% of the biomass (Hidaka et al., 2003). As well, distribution of euphausiids in French Polynesia oligotrophic waters showed an abundance maximum between 100 and 200 m depth (Legand et al., 1972). The agreement between vertical distribution patterns of S_v and those of myctophids and euphausiids indicates that these organisms possibly contribute to the nighttime S_v measured in the upper thermocline. Yet, gas-bearing siphonophores have not been sampled and could influence the scattering at such depth.

4.3.2. Influence of westerly wind events at 165°E

WWE dominate the intraseasonal variability in the western equatorial Pacific. They occur mostly between November and April and are stronger and more frequent during El Niño events. Local responses of the upper ocean are eastward equatorial surface jets, SST decreases, and deepening of the isothermal layer. The local biological response of the ocean is less well known and increases of surface chlorophyll have been observed during cruises or with satellite data. Siegel et al. (1995) proposed that such blooms were the result of vertical nutrient inputs because of enhanced vertical mixing. An alternative explanation is that nutrient- and chlorophyll-rich waters from the western warm pool, in particular from the upwelling north of New Guinea Island that develops when wind is westerly, may be advected eastward (Messié, 2006; Radenac et al., unpublished results). During the second half of 2002, very oligotrophic conditions prevailed east of 165°E, in particular at 170°W (Fig. 1b, Fig. 2). At 165°E, the ecosystem was moderately mesotrophic (surface chlorophyll around 0.1 mg m⁻³ or slightly higher) and the surface current was eastward (Fig. 8). Between July and December, nighttime S_v was about 4 dB higher than at the beginning of the year. The relative S_v minimum that flanked that period were concurrent with the passage of very oligotrophic waters of the eastern edge of the warm pool at 165°E, eastward in June 2002 and westward in February 2003. This pattern suggests that a water mass with distinct properties (nutrients, phytoplankton, and zooplankton and micronekton communities) occupied the western part of the equatorial warm pool during the 2002 El Niño while very oligotrophic waters persisted on its eastern edge. We can only speculate about mechanisms that maintain moderately mesotrophic conditions. SeaWiFS chlorophyll features indicate that advection of chlorophyll-rich (and nutrient-rich) water may significantly contribute (Radenac et al., unpublished results). Also, pulsating increases of nighttime S_v, simultaneous with or lagging WWE by a few days (Fig. 9b) suggest local influence of intense vertical mixing.

4.3.3. *Influence of moonlight*

We observed at 170°W that the delay between the dusk upward migration and downward movement progressively increased as the period between sunset and moonrise increased. This sequence is similar (except for the eclipse night) to the one described by Tarling et al. (1999) during 7 days around full moon in the Liguria Sea. Our time-series provide the opportunity to examine more precisely the evolution of the S_v signal during the entire lunar cycle and we found that patterns during the nights before full moon roughly mirrored those after full moon. Tarling et al. (1999) observed this behavior whatever the depth of food and concluded that it probably aimed at avoiding visual predators. They excluded a possible influence of endogenous rhythm because no sinking happened during darkness of an eclipse night. Among the main migrators (euphausiids and pteropods), only euphausiids responded to moonlight. Also, Roger (1974) observed that the time of euphausiid sinking in the southwest tropical Pacific was closely related to the time of moonrise during full moon periods. In the central equatorial Pacific, myctophids did not ascend during full moon periods (Legand et al., 1972). Based on this published literature, it appears that euphausiids and myctophids can be responsible for a part of the S_v modulations we observed in both equatorial ecosystems.

4.3.4. *Influence of stratification and food availability*

Our results suggest that thermocline depth strongly influences the vertical distribution of organisms, especially during the night. In oligotrophic conditions, downwelling Kelvin waves that depressed the thermocline in late 2002 at 170°W also deepened the subsurface high S_v layer. In the same way, the depth of the subsurface S_v maximum at 140°W strikingly followed the shoaling of the thermocline during the peak period of the 1997 El Niño. In mesotrophic conditions, the lower limit of the high S_v layer was lowered by downwelling Kelvin waves and matched variations of the thermocline depth at interannual scale as evidenced during the

pre- and post-El Niño periods in 1996-1999 at 140°W. This result is reminiscent of the deepening of the deep scattering layer west of 155°W associated with the deepening of the EUC and the zonal tilt of the thermocline during the Alizé trans-equatorial cruise (Grandperrin, 1969). The shallow thermal vertical structure following the 1997 El Niño conditions is unusual in the TAO/TRITON data. A similar event, marked with a shallow thermocline, occurred during the strong 1988-1989 La Niña when $Z_{20^{\circ}\text{C}}$ was around 50 m. The shallowest $Z_{20^{\circ}\text{C}}$ occurred in June-August 1998 during the bloom period. The migration pattern was uncommon as part of the organisms consistently found their daytime residence layer around 200 m during these months leading to anomalous high daytime S_v below $Z_{20^{\circ}\text{C}}$. Reasons for this are unclear. Organisms, whose daytime residence layer was below the transducer when the thermal structure was deeper, could adapt to a new environment and found better temperature and feeding conditions around 200 m. Also, species with reduced vertical migration may have developed because of favorable conditions during the bloom.

The vertical structure of chlorophyll is closely related to the vertical thermal structure in the equatorial Pacific and, therefore, we cannot fully separate the influence of stratification on S_v from that of food availability. The nitracline and the subsurface chlorophyll maximum coincide with the thermocline depth in the oligotrophic ecosystem while in the upwelling region, nitrate and phytoplankton are observed up to the surface. In both situations, nighttime vertical S_v distribution evokes the vertical distribution of phytoplankton. Phytoplankton are grazed by microzooplankton, which are ingested by mesozooplankton, which feed micronekton via the phytoplankton food chain (Legendre and Rivkin, 2005). Thus, chlorophyll-rich layers should sustain high microzooplankton and mesozooplankton and, in turn, higher micronekton biomass. Nighttime vertical S_v profiles may reflect the tendency for organisms to stop their migration at a preferred depth where they can feed easily: from the

middle of the thermocline to the surface in the upwelling zone and in the upper thermocline in the oligotrophic warm pool.

5. Concluding remarks

This study is an example of the use of single-frequency ADCPs to retrieve qualitative biological information at the same spatial and temporal scale as physical observations. In particular, we showed that different migrating patterns occur in oligotrophic and mesotrophic ecosystems and therefore, the limit between the warm pool and the upwelling region is also a transition in biomass and composition of zooplankton and micronekton species. We described the evolution of the migratory patterns during a lunar cycle and the response of the vertical S_v distribution to variations of the thermocline depth and, possibly, to food availability, at intra-seasonal and interannual scales. Finally, the complexity of the variations of the acoustic scattering in the eastern edge of the warm pool illustrates the great quantity of information the moored ADCP provided in vertical and temporal scales, information that cannot be resolved by conventional net hauls. However, we show that although some cues exist to explain observed S_v variations in the equatorial Pacific, many questions remain. More in situ data coupled to S_v estimates from acoustic scattering models are needed for obtaining quantitative biologically relevant variables and better understanding the behavior of zooplankton and micronekton along the equator, especially in the warm pool which does not appear as a very uniform oligotrophic region. Despite their limitations, long time-series of ADCP backscattering signal in the tropical Pacific offer a potentially valuable complement to more traditional approaches of studying mid-trophic levels and population dynamics.

Acknowledgements

We thank Robert Le Borgne for fruitful discussions at different stages of this study. We also thank reviewers for their incisive and useful comments that greatly helped to improve this paper. We thank the CNES for the financial support. PEP and MJM were funded by NOAA's Climate Program Office. PMEL publication No. 3163.

References

- Ashjian, C.J., Smith, S.L., Flagg, C.N., Wilson, C., 1998. Patterns and occurrence of diel vertical migration of zooplankton biomass in the Mid-Atlantic Bight described by an acoustic Doppler current profiler. *Continental Shelf Research* 18 (8), 831-858.
- Ashjian, C.J., Smith, S.L., Flagg, C.N., Idrisi, N., 2002. Distribution, annual cycle, and vertical migration of acoustically derived biomass in the Arabian Sea during 1994-1995. *Deep-Sea Research II* 49, 2377-2402.
- Ballón Soto, R.M., 2010. Acoustic study of macrozooplankton off Peru: biomass estimation, spatial patterns, impact of physical forcing and effect on forage fish distribution. Thèse de l'Université Montpellier II, 155p.
- Batchelder, H.P., VanKeuren, J.R., Vaillancourt, R., Swift, E., 1995. Spatial and temporal distributions of acoustically estimated zooplankton biomass near the Marine Light-Mixed Layers station (59°30'N, 21°00'W) in the north Atlantic in May 1991. *Journal of Geophysical Research* 100, 6549-6563.
- Chavez, F.P., Strutton, P.G., Friederich, G.E., Feely, R.A., Feldman, G.C., Foley, D.G., McPhaden, M.J., 1999. Biological and chemical response of the equatorial Pacific Ocean to the 1997-98 El Niño. *Science* 286, 2126-2131.
- Christian, J.R., Murtugudde, R., Ballabrera-Poy, J., McClain, C.R., 2004. A ribbon of dark water: phytoplankton blooms in the meanders of the Pacific North Equatorial Countercurrent. *Deep-Sea Research II* 51 (1-3) 209-228.

- Dam, H.G., Roman, M.R., Youngbluth, M.J., 1995. Downward export of respiratory carbon and dissolved inorganic nitrogen by diel-migrant mesozooplankton at the JGOFS Bermuda time-series station. *Deep-Sea Research I* 42 (7), 1187-1197.
- Dandonneau, Y., 1986. Monitoring the sea surface chlorophyll concentration in the tropical Pacific: consequences of the 1982-83 El Niño. *Fishery Bulletin* 84, 687-695.
- Fielding, S., Crisp, N., Allen, J.T., Hartman, M.C., Rabe, B., Roe, H.S.J., 2001. Mesoscale subduction at the Almeria-Oran front. Part 2: biophysical interactions. *Journal of Marine Systems* 30, 287-304.
- Fielding, S., Griffiths, G., Roe, H.S.J., 2004. The biological validation of ADCP acoustic backscatter through direct comparison with net samples and model predictions based on acoustic-scattering models. *ICES Journal of Marine Science* 61, 184-200.
- Fischer, J., Visbeck, M., 1993. Seasonal variation of the daily zooplankton migration in the Greenland Sea. *Deep-Sea Research* 40, 1547-1557.
- Flagg, C.N., Smith, S.L., 1989. Zooplankton abundance measurements from Acoustic Doppler Current Profilers. *OCEAN '89*, Marine Technology Society and IEEE, Seattle, WA, September 18-21, 6 pp.
- Flagg, C.N., Wirick, C.D., Smith, S.L., 1994. The interaction of phytoplankton, zooplankton, and currents from 15 months of continuous data in the Mid-Atlantic Bight. *Deep-Sea Research* 41, 411-435.
- Folt, C.L., Burns, C.W., 1999. Biological drivers of zooplankton patchiness. *Trends in Ecology and Evolution* 14 (8), 300-305.
- Francois, R.E., Garrison, G.R., 1982. Sound absorption based on ocean measurements. Part II: boric acid contribution and equation for total absorption. *Journal of Acoustical Society of America* 72 (6), 1879-1890.
- Gliwicz, Z.M., 1986. A lunar cycle in zooplankton. *Ecology* 67 (4), 883-897.

- Grandperrin, R., 1969. Couches diffusantes dans le Pacifique équatorial et sud-tropical. Cahiers ORSTOM Série Océanographie 7 (1), 99-112.
- Haney, J.F., 1988. Diel patterns of zooplankton behavior. Bulletin of Marine Science 43, 583-603.
- Hernández-León, S., 1998. Annual cycle of epiplanktonic copepods in Canary Island waters. Fisheries Oceanography 7 (3-4), 252-257.
- Heywood, K.J., 1996. Diel vertical migration of zooplankton in the Northeast Atlantic. Journal of Plankton Research 18, 163-184.
- Hidaka, K., Kawaguchi, K., Tanabe, T., Takahashi, M., Kubodera, T., 2003. Biomass and taxonomic composition of micronekton in the western tropical-subtropical Pacific. Fisheries Oceanography 12 (2), 112-125.
- Holliday, D.V., Pieper, R.E., 1995. Bioacoustical oceanography at high frequency. ICES Journal of Marine Science 52, 279-296.
- Jiang, S., Dickey, T.D., Steinberg, D.K., Madin, L.P., 2007. Temporal variability of zooplankton biomass from ADCP backscatter time series data at the Bermuda Testbed Mooring site. Deep-Sea Research I 54 (4), 608-636.
- Kaneko, A., Zhu, X.-H., Radenac, M.-H., 1996. Diurnal variability and quantification of subsurface sound scatterers in the western equatorial Pacific. Journal of Oceanography 5, 655-674.
- Kessler, W.S., 1990. Observations of long Rossby waves in the northern tropical Pacific. Journal of Geophysical Research 95, 5183-5217.
- Kuroda, Y., McPhaden, M.J., 1993. Variability in the western equatorial Pacific ocean during Japanese Pacific Climate Study Cruises in 1989 and 1990. Journal of Geophysical Research 98, 4747-4759.

- Landry, M.R., Barber, R.T., Bidigare, R.R., Chai, F., Coale, K.H., Dam, H.G., Lewis, M.R.,
Lindley, S.T., McCarthy, J.J., Roman, M.R., Stoecker, D.K., Verity, P.G., White, J.R.,
1997. Iron and grazing constraints on primary production in the central equatorial
Pacific: An EqPac synthesis. *Limnology and Oceanography* 42, 405-418.
- Lavery, A.C., Wiebe, P.H., Stanton, T.K., Lawson, G.L., Benfield, M.C., Copley, N.J., 2007.
Determining dominant scatterers of sound in mixed zooplankton populations. *Journal of*
the Acoustical Society of America 122, 3304-3326.
- Lawson, G.L., Wiebe, P.H., Stanton, T.K., Ashjian, C.J., 2008. Euphausiid distribution along
the Western Antarctic Peninsula - Part A: Development of robust multi-frequency
acoustic techniques to identify euphausiid aggregations and quantify euphausiid size,
abundance, and biomass. *Deep-Sea Research II* 55 (3-4), 412-431.
- Le Borgne, R., Rodier, M., 1997. Net zooplankton and the biological pump: a comparison
between the oligotrophic and mesotrophic equatorial Pacific. *Deep-Sea Research II* 44,
2003-2023.
- Le Borgne, R., Barber, R.T., Delcroix, T., Inoue, H.Y., Mackey, D.J., Rodier, M., 2002.
Pacific warm pool and divergence: temporal and zonal variations on the equator and
their effects on the biological pump. *Deep-Sea Research II* 49, 2471-2512.
- Legand, M., Bourret, P., Fourmanoir, P., Grandperrin, R., Guérédrat, J.-A., Michel, A.,
Rancurel, P., Repelin, R., Roger, C., 1972. Relations trophiques et distributions
verticales en milieu pélagique dans l'Océan Pacifique intertropical. *Cahiers ORSTOM*
Série Océanographie 10 (4), 303-343.
- Legendre L., Rivkin R.B., 2005. Integrating functional diversity, food web processes, and
biogeochemical carbon fluxes into a conceptual approach for modeling the upper ocean
in a high - CO world, *Journal of Geophysical Research* 110, C09S17,
doi:10.1029/2004JC002530.

- Lehodey, P., Bertignac, M., Hampton, J., Lewis, A., Picaut, J., 1997. El Niño Southern Oscillation and tuna in the western Pacific. *Nature* 389, 715-718.
- Lehodey, P., Murtugudde, R., Senina, I., 2010. A Spatial Ecosystem And Populations Dynamics Model (SEAPODYM) - Lower and mid-trophic levels. *Progress in Oceanography* 84, 69-84.
- León, R., Castro, L.R., Cáceres, M., 2008. Dispersal of *Munida gregaria* (Decapoda: Galatheidae) larvae in Patagonian channels of southern Chile. *ICES Journal of Marine Science* 65, 1131–1143.
- Longhurst, A.R., Bedo, A., Harrison, W.G., Head, E.J.H., Horne, E.P., Irwin, B., Morales, C., 1989. NFLUX: a test of vertical nitrogen flux by diel migrant biota. *Deep-Sea Research* 36 (11), 1705-1719.
- Mackey, D.J., Parslow, J., Higgins, H.W., Griffiths, F.B., Tilbrook, B., 1997. Plankton productivity and the carbon cycle in the western equatorial Pacific under ENSO and non-ENSO conditions. *Deep-Sea Research II* 44, 1951-1978.
- Madin, L.P., Horgan, E.F., Steinberg, D.K., 2001. Zooplankton at the Bermuda Atlantic Time-series Study (BATS) station: diel, seasonal and interannual variation in biomass, 1994–1998. *Deep-Sea Research II* 48 (8-9), 2063-2082.
- Mair A.M., Fernandes, P.G., Lebourges-Dhaussy, A., Brierley, A.S., 2005. An investigation into the zooplankton composition of a prominent 38-kHz scattering layer in the North Sea, *Journal of Plankton Research* 27 (7), 623-633.
- Marchal, E., Gerlotto, F., Stequert, B., 1993. On the relationship between scattering layer, thermal structure and tuna abundance in the Eastern Atlantic equatorial current system. *Oceanologica Acta* 16, 261-272.

- McClain, C.R., Feldman, G.C., Hooker, S.B., 2004. An overview of the SeaWiFS project and strategies for producing a climate research quality global ocean bio-optical time series. *Deep-Sea Research II* 51 (1-3), 5-42.
- McGehee, D.E., O'Driscoll, R.L., Traykovski, L.V.M., 1998. Effects of orientation on acoustic scattering from Antarctic krill at 120 kHz. *Deep-Sea Research II* 45 (7), 1273-1294.
- McPhaden, M.J., Busalacchi, A.J., Cheney, R., Donguy, J.-R., Gage, K.S., Halpern, D., Ji, M., Julian, P., Meyers, G., Mitchum, G.T., Niiler, P.P., Picaut, J., Reynolds, R.W., Smith, N., Takeuchi, K., 1998. The Tropical Ocean-Global Atmosphere observing system: A decade of progress. *Journal of Geophysical Research* 103, 14169-14240.
- McPhaden, M.J., 1999. Genesis and evolution of the 1997-98 El Niño. *Science* 283, 950-954.
- McPhaden, M.J., 2004. Evolution of the 2002/03 El Niño. *Bulletin of the American Meteorological Society* 85, 677-695.
- Messié, M., 2006. Contrôle de la dynamique de la biomasse phytoplanctonique dans le Pacifique tropical ouest. Thèse de doctorat de l'Université Toulouse 3, Océanographie, 263 pp.
- Messié, M., Radenac, M.-H., 2006. Seasonal variability of the surface chlorophyll in the western tropical Pacific from SeaWiFS data. *Deep Sea Research I* 53 (10), 1581-1600.
- Munk, P., Kiørboe, T., Christensen, V., 1989. Vertical migrations of herring, *Clupea harengus*, larvae in relation to light and prey distribution. *Environmental Biology of Fishes* 26(2), 87-96.
- Murtugudde, R.G., Signorini, S.R., Christian, J.R., Busalacchi, A.J., McClain, C.R., Picaut, J., 1999. Ocean color variability of the tropical Indo-Pacific basin observed by SeaWiFS during 1997-98. *Journal of Geophysical Research* 104, 18351-18365.

- 767 Navarette, C., 1998. Dynamique du phytoplancton en océan équatorial: mesures
 1
 2 768 cytométriques et mesures isotopiques durant la campagne FLUPAC, en octobre 1994
 3
 4 769 dans la partie ouest du Pacifique. Thèse de Doctorat de l'Université Paris VI, 313 pp.
 5
 6
 7 770 Ona, E., Mitson, R.B., 1996. Acoustic sampling and signal processing near the seabed: the
 8
 9 771 deadzone revisited. ICES Journal of Marine Science, 53, 677-690.
 10
 11
 12 772 Pinot, J.-M., Jansá, J., 2001. Time variability of acoustic backscatter from zooplankton in the
 13
 14 773 Ibiza Channel (western Mediterranean). Deep-Sea Research I 48, 1651-1670.
 15
 16
 17 774 Plimpton, P.E., Freitag, H.P., McPhaden, M.J., 2004. Processing of subsurface ADCP Data in
 18
 19 775 the Equatorial Pacific. NOAA Technical Memorandum OAR PMEL-125, 41 pp.
 20
 21
 22 776 Plimpton, P.E., Freitag, H.P., McPhaden, M.J., 1997. ADCP Velocity errors from pelagic fish
 23
 24 777 schooling around equatorial moorings. Journal of Atmospheric and Oceanic Technology
 25
 26 778 14 (5), 1212-1223.
 27
 28
 29 779 Plueddemann, A.J., Pinkel, R., 1989. Characterization of the patterns of diel migration using a
 30
 31 780 Doppler sonar. Deep-Sea Research 36, 509-530.
 32
 33
 34 781 Radenac, M.-H., Rodier, M., 1996. Nitrate and chlorophyll distributions in relation to
 35
 36 782 thermohaline and current structures in the western tropical Pacific during 1985-1989.
 37
 38 783 Deep-Sea Research II 43, 725-752.
 39
 40
 41 784 Radenac, M.-H., Menkes, C., Vialard, J., Moulin, C., Dandonneau, Y., Delcroix, T., Dupouy,
 42
 43 785 C., Stoens, A., Deschamps, P.-Y., 2001. Modeled and observed impacts of the 1997-
 44
 45 786 1998 El Niño on nitrate and new production in the equatorial Pacific. Journal of
 46
 47 787 Geophysical Research 106, 26879-26898.
 48
 49
 50
 51 788 Radenac, M.-H., Dandonneau, Y., Blanke, B., 2005. Displacements and transformations of
 52
 53 789 nitrate-rich and nitrate-poor water masses in the tropical Pacific during the 1997 El
 54
 55 790 Niño, Ocean Dynamics 55 (1), 34-46.
 56
 57
 58
 59
 60
 61
 62
 63
 64
 65

- RD Instruments, 1990. Calculating absolute backscatter. Technical Bulletin ADCP-90-04, RD Instruments, San Diego, CA, USA, 24pp.
- Ressler, P.H., 2002. Acoustic backscatter measurements with a 153 kHz ADCP in the northeastern Gulf of Mexico: determination of dominant zooplankton and micronekton scatterers. *Deep-Sea Research I* 49, 2035-2051.
- Reynolds, R.W., Rayner, N.A., Smith, T.M., Stokes, D.C., Wang, W., 2002. An improved *in situ* and satellite SST analysis for climate. *Journal of Climate* 15, 1609-1625.
- Rodier, M., Eldin, G., Le Borgne, R., 2000. The western boundary of the equatorial Pacific upwelling: some consequences of climatic variability on hydrological and planktonic properties. *Journal of Oceanography* 56, 463-471.
- Roger, C., 1971. Distribution verticale des euphausiacés (crustacés) dans les courants équatoriaux de l'océan Pacifique. *Marine Biology* 10 (2), 134-144.
- Roger, C., 1974. Influence de la phase et de l'éclairement lunaire sur les répartitions verticales nocturnes superficielles de crustacés macro-planctoniques (*Euphausiacea*). *Cahiers ORSTOM Série Océanographie* 12 (3), 159-171.
- Ryan, J.P., Polito, P.S., Strutton, P.G., Chavez, F.P., 2002. Unusual large-scale phytoplankton blooms in the equatorial Pacific. *Progress in Oceanography* 55 (3), 263-285.
- Schott F., Johns, W., 1987. Half-year-long measurements with a buoy-mounted acoustic Doppler current profiler in the Somali current, *Journal of Geophysical Research* 92 (C5), 5169-5176.
- Serra, Y., McPhaden, M.J., 2004: In situ observations of the diurnal variability in rainfall over the tropical Atlantic and Pacific Oceans. *Journal of Climate* 17, 3496–3509.
- Siegel, D.A., Ohlman, J.C., Washburn, L., Bidigare, R.R., Nosse, C.T., Fields, E., Zhou, Y., 1995. Solar radiation, phytoplankton pigments and the radiant heating of the equatorial Pacific warm pool. *Journal of Geophysical Research* 100, 4885-4891.

- Stanton, T.K., Wiebe, P.H., Chu, D., Benfield, M.C., Scanlon, L., Martin, L., Eastwood, R.L.,
1994. On acoustic estimates of zooplankton biomass. ICES Journal of Marine Science,
51, 505-512.
- Steinberg, D.K., Goldthwait, S.A., Hansell, D.A., 2002. Zooplankton vertical migration and
the active transport of dissolved organic and inorganic nitrogen in the Sargasso Sea.
Deep-Sea Research I 49 (8), 1445-1461.
- Stoens, A., Menkes, C., Radenac, M.-H., Grima, N., Dandonneau, Y., Eldin, G., Memery, L.,
Navarette, C., André, J.-M., Moutin, T., Raimbault, P., 1999. The coupled physical-new
production system in the equatorial Pacific during the 1992-1995 El Niño. Journal of
Geophysical Research 104, 3323-3339.
- Strutton, P.G., Chavez, F.P., 2000. Primary productivity in the equatorial Pacific during the
1997-98 El Niño. Journal of Geophysical Research 105, 26089-26101.
- Tarling, G.A., Buchholz, F., Matthews, J.B.L., 1999. The effect of a lunar eclipse on the
vertical migration behaviour of *Meganycitiphanes norvegica* (Crustacea: Euphausiacea)
in the Ligurian Sea. Journal of Plankton Research 21 (8), 1475-1488.
- Turk, D., McPhaden, M.J., Busalacchi, A.J., and Lewis, M.R., 2001. Remotely sensed
biological production in the equatorial Pacific. Science 293, 471-474.
- Vélez-Belchí, P., Allen, J.T., Strass, V.H., 2002. A new way to look at mesoscale zooplankton
distributions: an application at the Antarctic Polar Front. Deep-Sea Research II 49 (18),
3917-3929.
- Velsch, J.-P., Champalbert, G., 1994. Rythmes d'activité natatoire chez *Meganycitiphanes*
norvegica (Crustacea, Euphausiacea). Comptes Rendus de l'Académie des Sciences
Paris, Sciences de la Vie 317, 857-862.

- Wade, I.P., Heywood, K.J., 2001. Acoustic backscatter observations of zooplankton abundance and behavior and the influence of oceanic fronts in the northeast Atlantic. *Deep-Sea Research II* 48, 899-924.
- Wang, X.J., Behrenfeld, M., Le Borgne, R., Murtugudde, R., Boss, E., 2009. Regulation of phytoplankton carbon to chlorophyll ratio by light, nutrients and temperature in the equatorial Pacific Ocean: a basin-scale model. *Biogeosciences* 6, 391-404.
- Warren, J.D., Stanton, T.K., McGehee, D.E., Chu, D., 2002. Effect of animal orientation on acoustic estimates of zooplankton properties , *IEEE Journal of Oceanic Engineering*, 27 (1), 130-138.
- Wiebe, P.H., Greene, C.H., Stanton, T.K., Burczynski, J., 1990. Sound scattering by live zooplankton and micronekton: empirical studies with a dual-beam acoustical system. *Journal of Acoustical Society of America* 88, 2346-2360.
- Wiebe P.H., Mountain, D., Stanton, T.K., Greene, C., Lough, G., Kaartvedt, S., Manning, J., Dawson, J., Martin, L., Copley, N., 1996. Acoustical study of the spatial distribution of plankton on Georges Bank and the relation of volume backscattering strength to the taxonomic composition of the plankton. *Deep-Sea Research II* 43, 1971-2001.

position	deployment	time period
0°, 140°W	ca2	4 Sept. 1996 – 21 Oct. 1997
	ca3	21 Oct. 1997 – 27 Sept. 1998
	ca4	28 Sept. 1998 – 19 Sept. 1999
0°, 170°W	ka7	20 Jun. 2002 – 29 Jun. 2003
	ka8	30 Jun. 2003 – 9 Jul. 2004
0°, 165°E	wa3	4 Nov. 2001 – 5 Nov. 2002
	wa4	6 Nov. 2002 – 21 Nov. 2003

Table 1. ADCP deployments along the equator.

	mesotr.	oligotr.
170°W	Feb. 2003 – Jun. 2004	Sep. – Dec. 2002
night	-49.4	-56.1
day	-58.2	-61.8
140°W	Sep. 1996 – Sep. 1997	Nov. – Dec. 1997
night	-49.5	-55.9
day	-59.0	-63.5

Table 2. Mean nighttime and daytime S_v (dB) averaged above $Z_{20^{\circ}\text{C}}$ in oligotrophic and mesotrophic conditions at 170°W and 140°W.

Figure captions

Fig.1. (a) SeaWiFS chlorophyll in May 2002. The dark line is the 0.1 mg m^{-3} isoline, black squares indicate the 3 ADCP mooring sites. Longitude–time diagrams of (b) eight-day SeaWiFS chlorophyll averaged between 1°S and 1°N and (c) five-day average anomalies of the 20°C isotherm depth from the TAO/TRITON equatorial moorings. The dark line is the 29°C surface isotherm derived from Reynolds (2002) and TMI. Vertical black lines mark the duration of the ADCP time-series at 165°E , 170°W , and 140°W .

Fig.2. Time evolution at 0° , 170°W of the SeaWiFS chlorophyll (a), the vertical structure of nighttime (b) and daytime (c) S_v . The dashed line in (a) marks the 0.1 mg m^{-3} chlorophyll concentration. The upper (lower) black lines superimposed on S_v distribution in (b) and (c) are the 29°C (20°C) isotherm depths. Vertical dashed lines in (b) indicate full moon nights.

Fig. 3. Top panels: example of mesotrophic conditions at the 0° , 170°W mooring in June 2003. (a) Two successive S_v diel cycles. (b) Vertical profiles of the nighttime S_v (thick line), daytime S_v (thin line), and temperature (dashed line). Bottom panels: the same for oligotrophic conditions in October 2002. In (a) and (c), contour interval is every 2 dB; thick contours are the -70, -60, and -50 dB. Time is local time.

Fig.4. Evolution of the nighttime S_v (dB) at 40 m (a) and at 170 m (b). Dashed lines indicate full moon nights.

Fig. 5. Influence of the moon on the S_v diel cycles of September 2003 (local time) at 0° , 170°W in the mesotrophic regime. New moon (NM), first quarter (FQ), full moon (FM), and

last quarter (LQ) are indicated. Heavy black lines indicate hours of darkness between sunrise (06:00LT) and moonset before full moon, and between sunset (18:00 LT) and moonrise after full moon. Contour interval is 2 dB; dark lines are the -70, -60, and -50 dB levels.

Fig.6. Time evolution at 0° , 140°W of the SeaWiFS chlorophyll and TAO/TRITON SST (a), the vertical structure of nighttime (b) and daytime (c) S_v . The dashed line in (a) marks the 0.1 mg m^{-3} chlorophyll concentration. The upper (lower) black line superimposed on S_v distribution in (b) and (c) is the 29°C (20°C) isotherm depth. Vertical dashed lines in (b) indicate full moon nights.

Fig. 7. S_v diel cycles (dB) during the bloom period at 0° , 140°W in July 1998. Time is local time. Contour interval is 2 dB; dark contours are the -70, -60, and -50 dB isolines.

Fig.8. Time evolution at 0° , 165°E of SeaWiFS chlorophyll (black line) and zonal wind speed (TAO: red line; QuickScat: dashed red line) (a), the vertical structure of nighttime (b) and daytime (c) S_v , and the zonal current component (d). The dashed line in (a) marks the 0.1 mg m^{-3} chlorophyll concentration and the 0.0 m s^{-1} zonal wind speed. The upper (lower) black line in (b), (c), and (d) is the 29°C (20°C) isotherm depth. Vertical dashed lines in (b) indicate full moon nights.

Fig. 9. Temporal evolution at 0° , 165°E during the mild 2002 El Niño of nighttime S_v averaged above $Z_{29^{\circ}\text{C}}$ (black line) and of (a) the zonal current at 50 m (red line); (b) the same zonal wind speed as in Fig. 8 (red lines).

Figure
[Click here to download Figure: Fig1.eps](#)

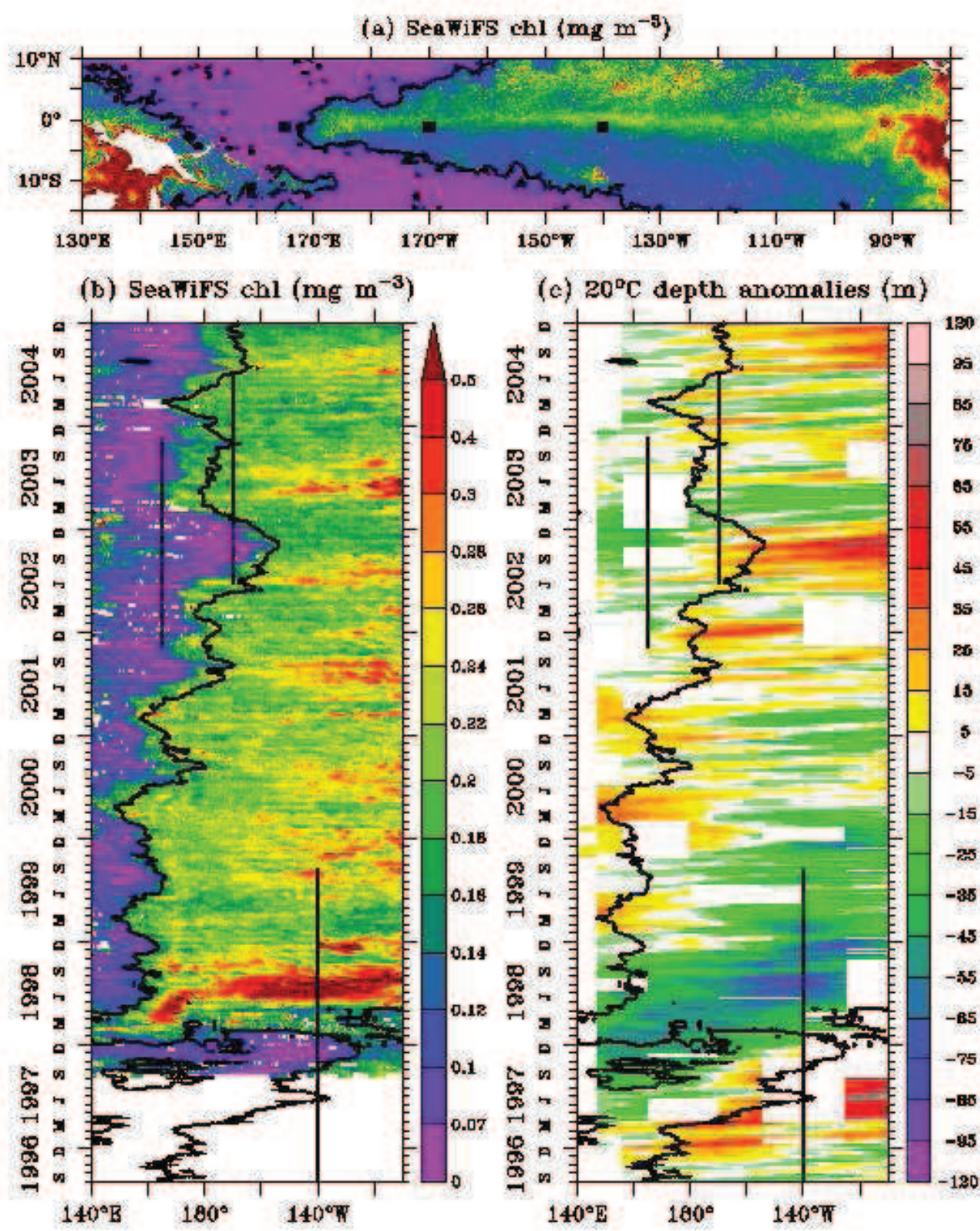


Figure
[Click here to download Figure: Fig2.eps](#)

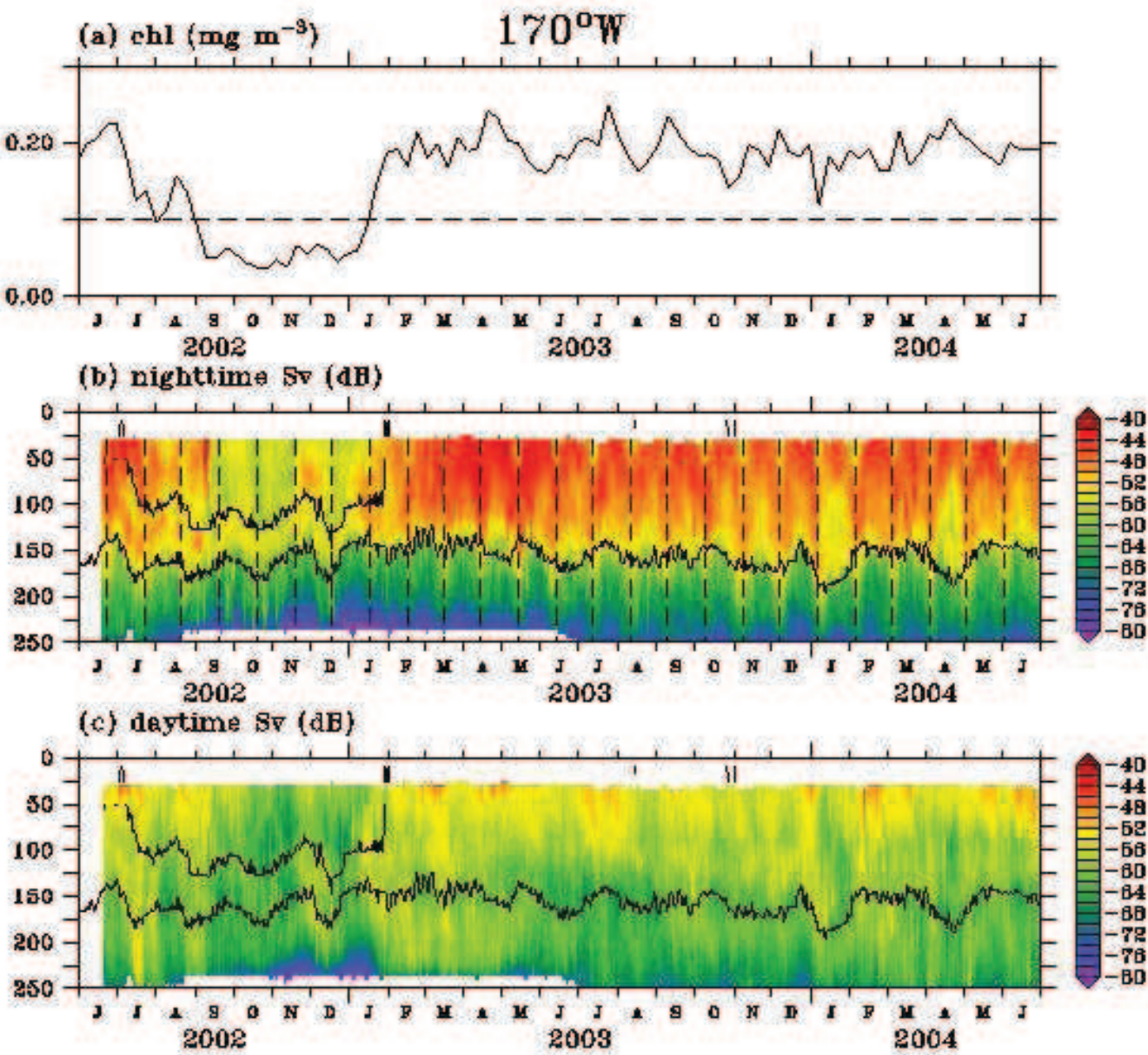


Figure
[Click here to download Figure: Fig3.eps](#)

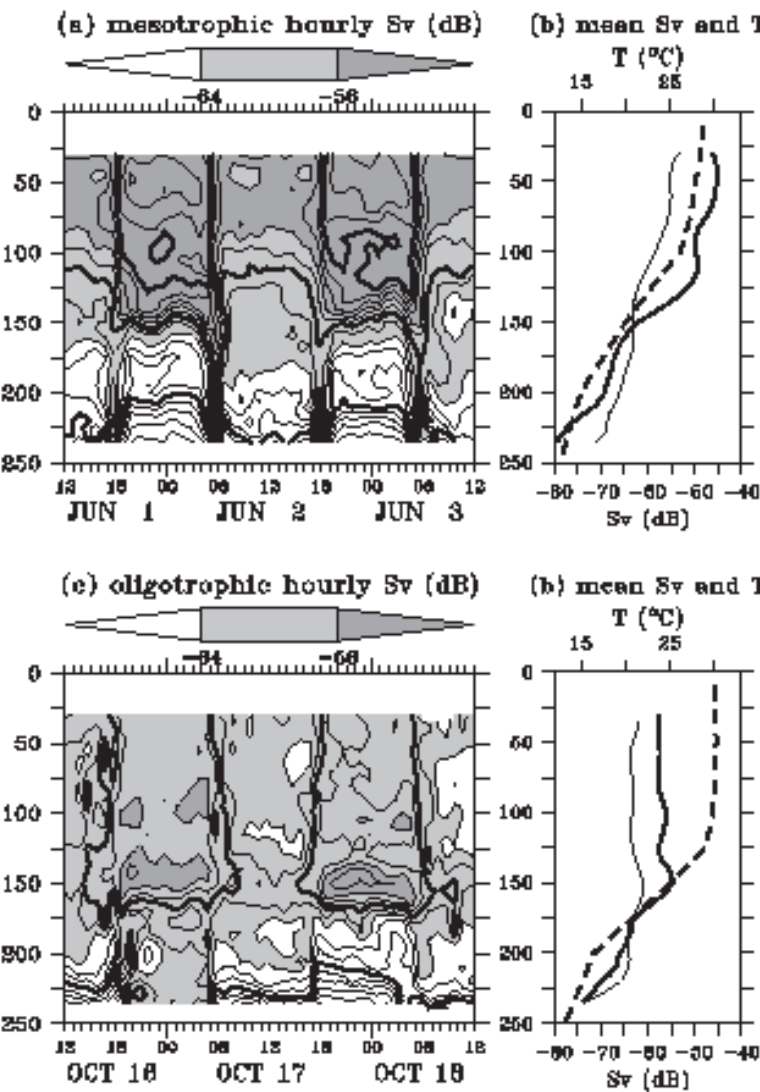


Figure
[Click here to download Figure: Fig4.eps](#)

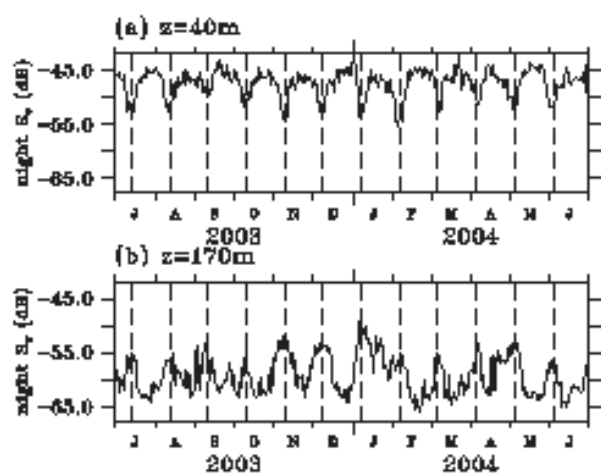


Figure
[Click here to download Figure: Fig5.eps](#)

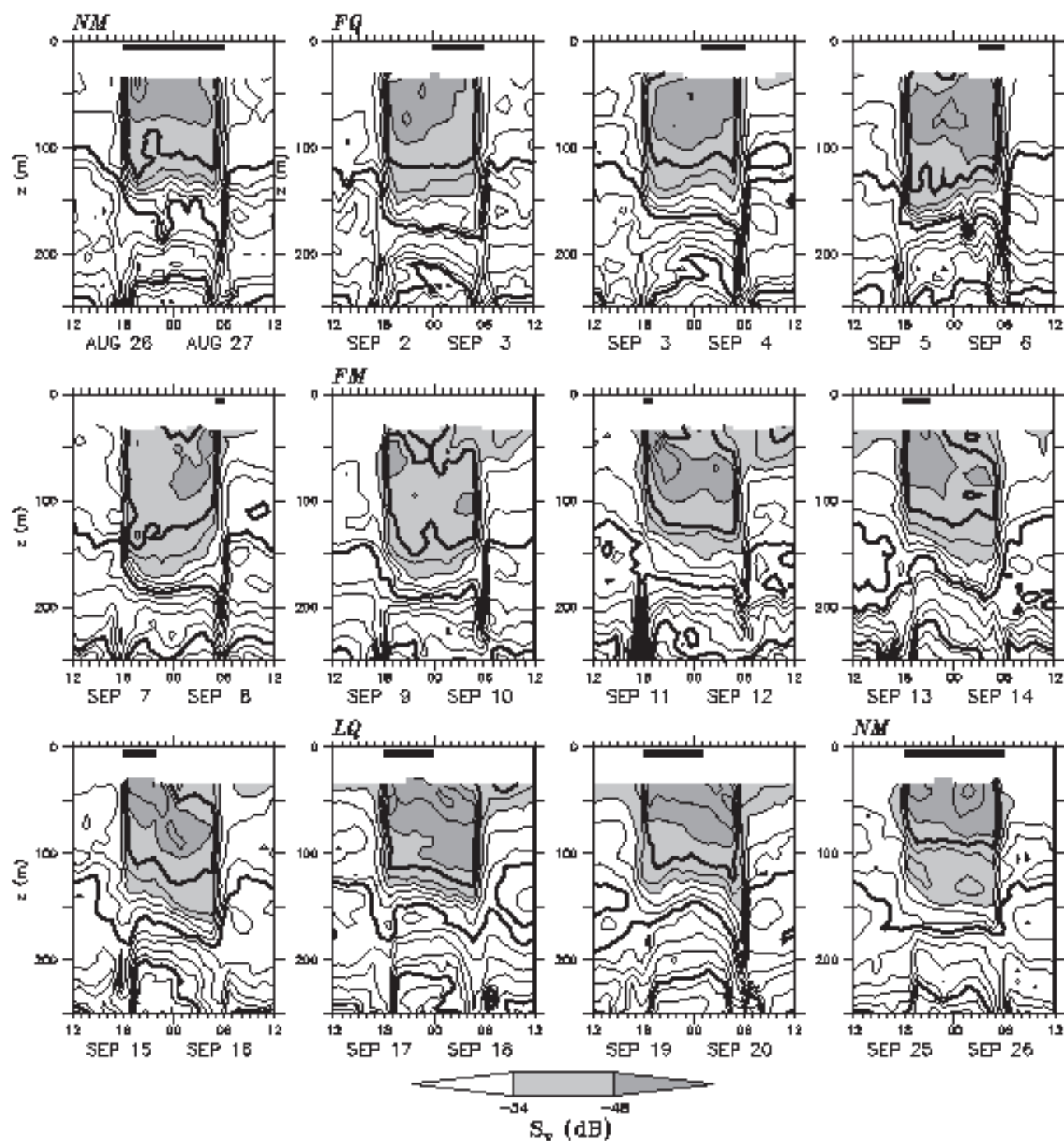


Figure
[Click here to download Figure: Fig6.eps](#)

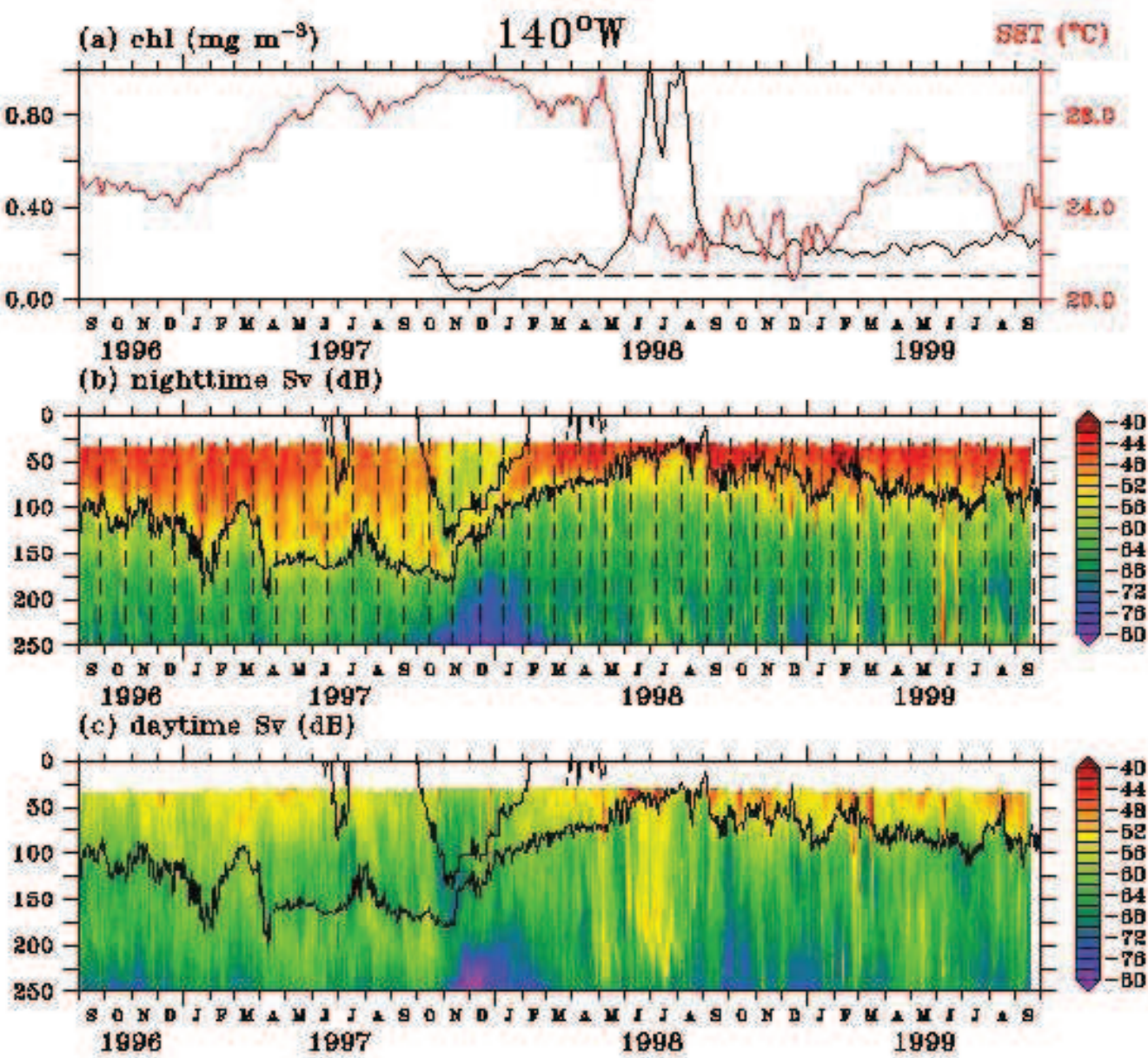


Figure
[Click here to download Figure: Fig7.eps](#)

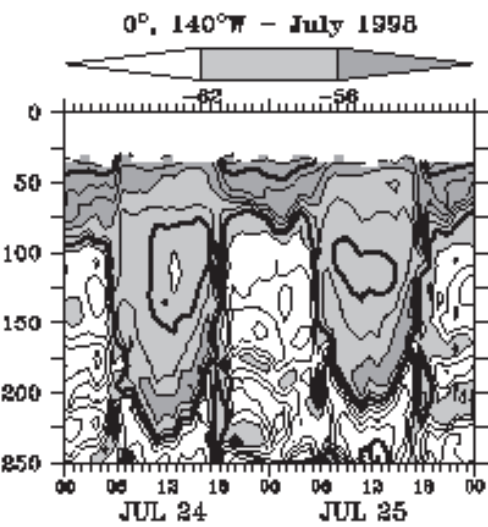


Figure
[Click here to download Figure: Fig8.eps](#)

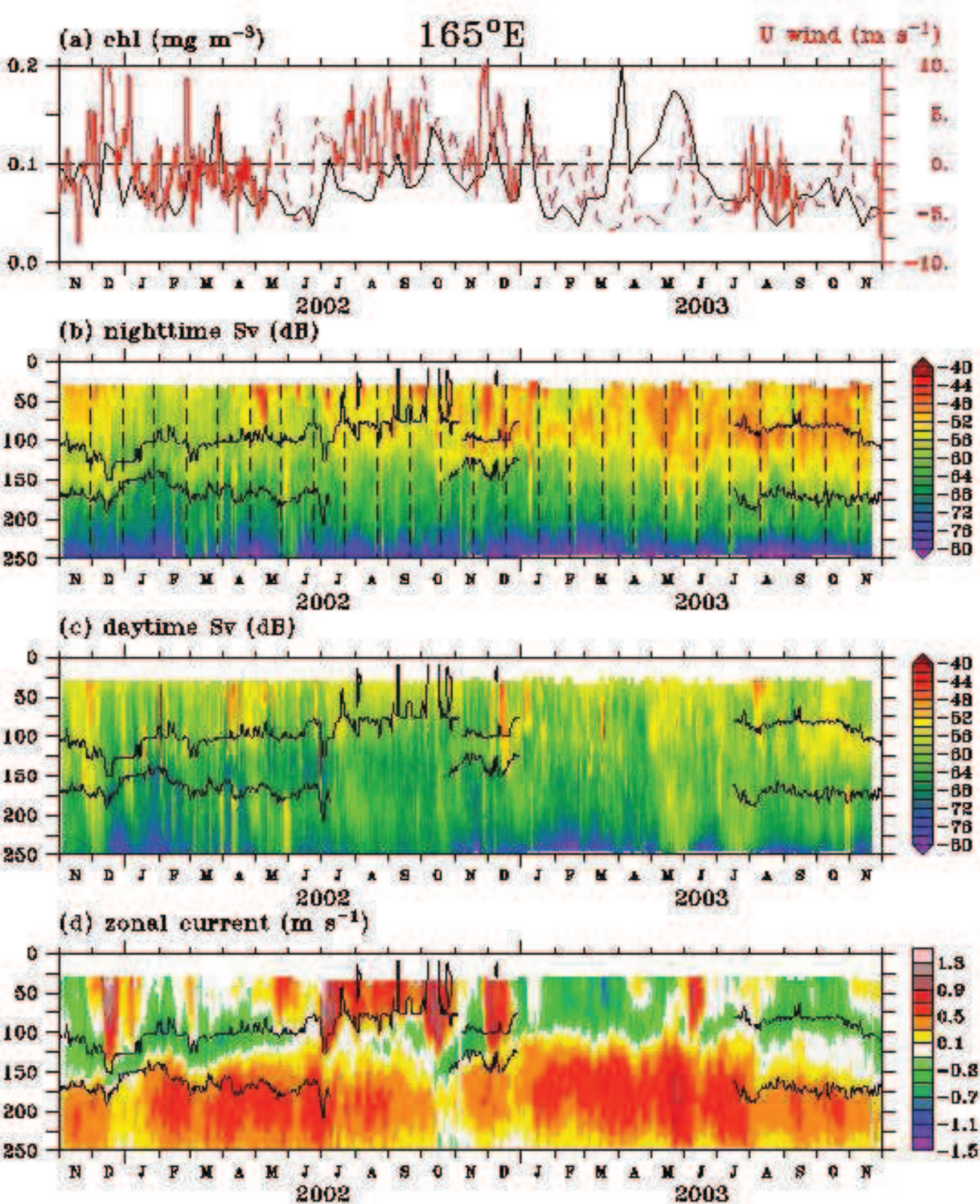


Figure
[Click here to download Figure: Fig9.eps](#)

